Supporting Information to the manuscript

JANUS DISCS

by Andreas Walther, Xavier André, Markus Drechsler, Volker Abetz, Axel H. E. Müller

1. Experimental Part

Materials. All solvents and reagents were obtained from Merck or Aldrich in p.a. grade and used without further treatment except for the following ones. Zipcone UA was purchased from ABCR. Decane (p.a., Aldrich) and Isooctane (p.a., Aldrich) were treated with *sec*-butyl lithium and distilled. THF (p.a. Merck) was treated with *sec*-butyl lithium at low temperatures and distilled. Cyclohexane (Merck) and acetonitrile (Aldrich) were obtained in HPLC grade and used directly.

Synthesis. The anionic polymerization of the polystyrene-*block*-polybutadiene-*block*-poly(*tert*-butyl methacrylate) (SBT) terpolymers was conducted in a similar way as reported elsewhere.[1, 2]

Crosslinking with AIBN / Thiol-Polyene process. AIBN (5 wt%, relative to the mass of the SBT terpolymer), trimethylolpropane mercaptopropionate (TRIS, 0 - 5 wt%) and SBT terpolymer were dissolved in $CHCl_3$ and the film casting process was allowed to take place in a solvent vapour filled desiccator for about two weeks. Afterwards, the film was dried in vacuo at RT for 24 h and crosslinked at 80 °C for 48 h. Subsequently, the film was purified by Soxhlet extraction with THF for 24 h yielding a soluble fraction and an insoluble fraction. The insoluble fraction was subjected to a sonication treatment.

Cold vulcanization. A solvent-cast film was introduced into a reaction vessel and swollen in solvent (decane or isooctane) for a certain period of time (typically: 12 – 48 h). Afterwards, the calculated amount of S_2Cl_2 (typically: 1.5 – 5 vol%) was introduced with a syringe and the crosslinking was allowed to take place for 12 - 48 h at room temperature. After the reaction, the film was washed with several aprotic non-solvents, e.g. acetonitrile and isooctane. Subsequently, the film was purified by Soxhlet extraction with THF for 24 h yielding a

soluble and an insoluble fraction. The insoluble fraction was subjected to a sonication treatment.

Sonication. The product underwent ultrasonic treatment using a Branson model-250 digital sonifier, equipped with 1/8 in. diameter tapered microtip, at various amplitudes (200 watt at 100% amplitude). For this purpose, a dispersion of insoluble crosslinked material (c = 0.3 - 1 mg/mL) in THF was allowed to stand at room temperature for several hours to ensure good swelling of the material. Afterwards, it was subjected to the sonication treatment in a temperature controlled cell. The on/off cycle times were typically in the range of 2s/2s and 2s/10s, depending on the amplitude used.

TEM imaging of embedded Janus discs. 10 – 30 mg of Janus discs were dissolved in 1 ml of THF or acetone and added to a vial containing 0.1 – 0.3 mL of Zipcone UA (photo-crosslinkable silicon oil). After rapid evaporation of the solvent, the silicon oil was crosslinked using a standard UV lamp for 1h. Subsequently, the solidified block was microtome cut and the ultrathin sections were stained with OsO_4 prior to TEM imaging.

GPC-MALS measurements were performed at room temperature using a GPC equipped with a Wyatt Technology DAWN DSP-F multi-angle light scattering detector (He-Ne Laser; λ = 632.8 nm) and a Shodex-RI-71 refractive index detector. Three 30 cm PSS SDV columns (10^4, 10^5, and 10^6 Å) were used with THF as eluent at a flow rate of 1 mL/min. Data evaluation was performed with the Astra Software package.

NMR. ^{1}H- and ^{13}C-NMR spectra were obtained on a Bruker AC 250 at an operating frequency of 250 MHz and 62.5 MHz, respectively. Various deuterated solvents (Deutero GmbH) were used depending on the solubility of the samples. As an internal standard, the residual proton signal of the deuterated solvent was used.

Dynamic Light Scattering (DLS). Dynamic light scattering was performed on an ALV DLS/SLS-SP 5022F compact goniometer system with an ALV 5000/E cross-correlator and a He–Ne laser (λ_0 = 632.8 nm). Prior to the light scattering measurements the sample solutions were filtered using Millipore or Roth filters (housing: polypropylene, membrane: polytetrafluoroethylene) with a pore size of 5 μm. All samples were analyzed at high dilution. The data evaluation of the dynamic light scattering measurements was performed with the CONTIN algorithm[3] and the values of the hydrodynamic radii were obtained after extrapolating the angle-dependent scattering data to $q^2 \rightarrow 0$.[4]

Small Angle X-ray Scattering (SAXS). The SAXS measurements in this work were carried out at the ID02A high-brilliance beamline at the European Synchrotron Radiation Facility (ESRF, Grenoble, France). The operating energy range was 12.5 keV, corresponding to a wavelength of 0.1 nm, at which the highest photon flux is obtained. The detector system with a standard two-dimensional SAXS camera is housed in a 10 m evacuated flight tube. For the experiments an image intensified CCD detector is used, which can handle the full X-ray flux. Prior to data analysis, background scattering was subtracted from the data and corrections were made for spatial distortions and for the detector efficiency. The data evaluation was performed with home-written software.

Scanning Electron Microscopy (SEM). SEM was performed using a LEO 1530 Gemini instrument equipped with a field emission cathode with a lateral resolution of approximately 2 nm. The acceleration voltage was chosen between 0.5 and 3 kV. Statistical analysis of the size distribution of the particles was performed with ImageJ V1.32 and ImageTool V3.0.

Transmission Electron Microscopy (TEM). The bulk morphologies of the SBT triblock terpolymer were examined using TEM. Films (around 1 mm thick) were cast from 5% (w/w) solutions in $CHCl_3$ and allowed to evaporate slowly for 2 weeks. The as-cast films were dried for 1 day in vacuum at room temperature and then annealed at 80 °C for 1 - 5 days. Thin sections were cut at room temperature using a Reichert-Jung Ultracut E microtome equipped with a diamond knife. To enhance the electron density contrast between the three blocks, the sections were exposed to OsO_4 vapour for 60 s, which leads to a preferential staining of the polybutadiene block appearing black. Bright-field TEM was performed on Zeiss CEM 902 and LEO 922 OMEGA electron microscopes operated at 80 kV and 200 kV, respectively.

For **cryogenic transmission electron microscopy (cryo-TEM)** studies, a drop of the sample dissolved in THF was put on a lacey transmission electron microscopy (TEM) grid, where most of the liquid was removed with blotting paper, leaving a thin film stretched over the lace. The specimens were instantly vitrifed by rapid immersion into liquid nitrogen and cooled to approximately 90 K by liquid nitrogen in a temperature controlled freezing unit (Zeiss Cryobox, Zeiss NTS GmbH, Oberkochen, Germany). The temperature was monitored and kept constant in the chamber during all of the sample preparation steps. After freezing the specimens, the specimen was inserted into a cryo-transfer holder (CT3500, Gatan, München, Germany) and transferred to a Zeiss EM922 EF-TEM instrument. Examinations were carried out at temperatures around 90 K. The transmission electron microscope was operated at an acceleration voltage of 200 kV. Zero-loss filtered images ($\Delta E = 0$ eV) were taken under

reduced dose conditions (100-1000 e/nm^2). All images were registered digitally by a bottom mounted CCD camera system (Ultrascan 1000, Gatan) combined and processed with a digital imaging processing system (Gatan Digital Micrograph 3.9 for GMS 1.4).

Scanning Force Microscopy (SFM). SFM images were taken on a Digital Instruments Dimension 3100 microscope or on a Veeco Multimode operated in Tapping Mode. The standard silicon nitride probes and super-sharp probes were driven at 3 % offset below their resonance frequencies in the range of 250 - 350 kHz. According to the distributor of the tips, the normal tips and the super sharp tips possess finite tip sizes with radii of 10 - 20 nm and 2 nm, respectively. Offline data processing was done using the Nanoscope Software (V 5.13r10sr1 and V6r2.1) and Gwyddion 1.12.

Pendant Drop Tensiometer isotherms of the interfacial tension were measured on a Dataphysics OCA 20 tensiometer at room temperature. The particle concentration was in the range of 1 mg/ml to 0.1 mg/ml. The shape of the pendant drop was recorded using a CCD camera and the fitting was performed with the Dataphysics software package.

2. Crosslinking

The crosslinking of the polybutadiene part was accomplished via two ways, the thiol-polyene procedure and by cold vulcanization. The detailed and carefully optimized procedures for the crosslinking of the block terpolymer templates will be published separately. However, a short overview of the experiments is provided in the following.

Cold vulcanization is the reaction of double bonds with S_2Cl_2 in the swollen state. Since the morphologies of the block terpolymers react very sensitively to changes in solvent quality, the conditions were carefully optimized in order to ensure the integrity of the morphology at all stages of the process, i.e. after the addition of swelling solvent and crosslinking agent. Among the suitable solvents and solvent combinations investigated, only decane and isooctane can be used to swell the morphology as they do not alter the microphase-separated structure in any undesired fashion. Additionally, the concentration of the crosslinking agent, S_2Cl_2, may not exceed a certain level, as otherwise an unwanted transition to a core-shell cylinder morphology with P*t*BMA as matrix can take place. However, after careful screening of the experimental conditions, the cold vulcanization was performed successfully.

The alternative crosslinking method using AIBN, or its optimized process, the thiol-polyene reaction[5], can be performed in a more straightforward manner. According to the work of Decker et al.[6-9], the crosslinking of polybutadiene domains with AIBN in combination with trimethylolpropane mercaptopropionate (TRIS), a trifunctional crosslinking agent, leads to an increased fraction of insoluble material (thiol-polyene reaction). This is due to the fact, that TRIS can act as transfer agent and is also able to react with the 1,4-polybutadiene moieties which are usually not attacked during a normal radical crosslinking. Hence, it was taken advantage of this beneficial influence and the addition of the trifunctional thiol led to a larger fraction of insoluble material. Before carrying out the crosslinking, TEM images were recorded in order to assure the presence of lamellar morphologies and it was found that film casting in presence of AIBN and TRIS has no influence on the development of the lamellar (ll) morphology. Hence, it is unambiguous that annealing such structures leads to a rapid crosslinking, preserving the microphase-separated morphology. The success of this strategy was confirmed by TEM, which showed the clear persistence of the lamellar morphologies after crosslinking (see figure S-1).

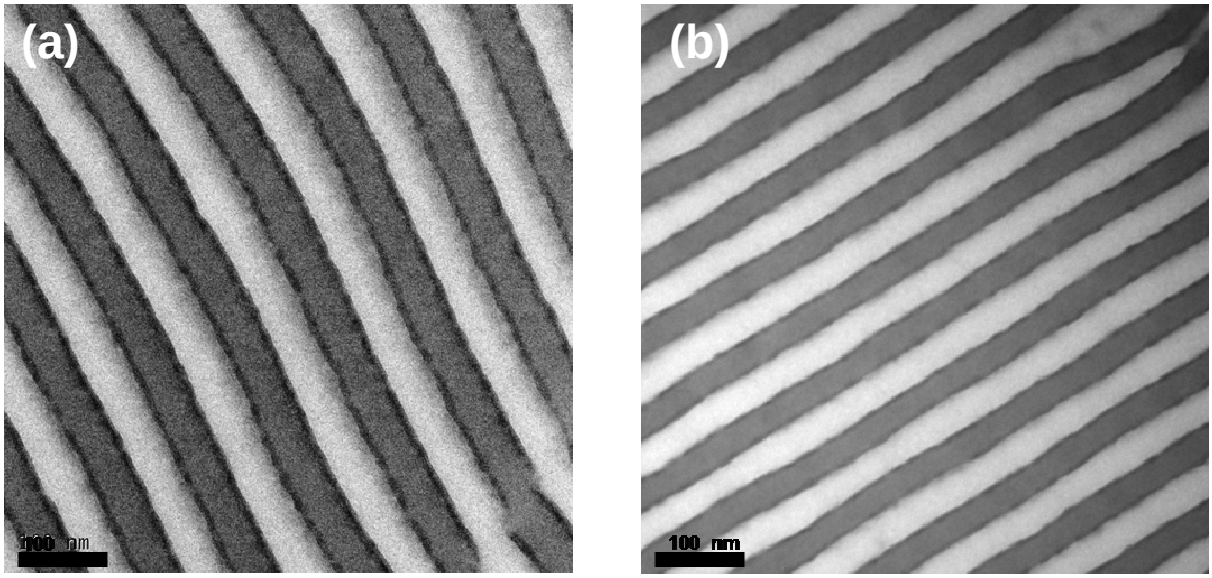

Figure S-1. Transmission electron micrograph of ultrathin sections of SBT-1 films, which were crosslinked with S_2Cl_2 after swelling in isooctane (a) or an AIBN/TRIS mixture (b). Residual uncrosslinked double bonds were stained with OsO_4 to improve the contrast.

3. Spectroscopic characterization by ^{1}H-NMR

Spectroscopic characterization of the SBT precursor terpolymer sample and a Janus dics sample obtained after sonication of a template which was crosslinked with 5 wt% AIBN in the presence of 5 wt% TRIS.

Clearly, both spectra show the presence of styrene (a) and *t*-butyl methacrylate units (d) before and after the template-assisted preparation of Janus discs. Herewith, the proposed composition of the outer sides can be confirmed. Additionally, the strong and successful crosslinking of the inner polybutadiene layer of the template can be deduced from the diminishing peaks b and c, corresponding to the unsaturated polybutadiene moieties.

The NMR peaks appear broader after the crosslinking and sonication due to their origin from larger structures with lower flexibility as compared to the initial terpolymer spectrum.

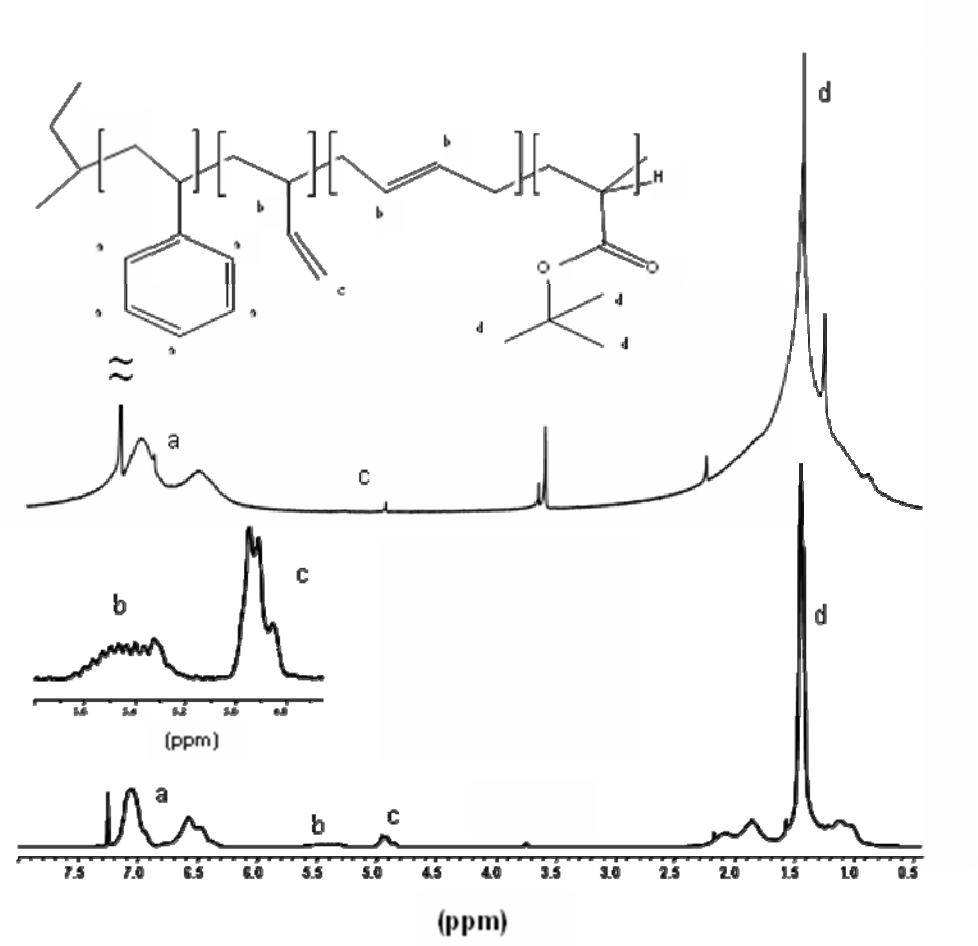

Figure S-2: ^{1}H-NMR spectra of SBT-1 (lower) and a Janus disc sample obtained after sonication of a crosslinked SBT-1 template (upper).

4. Height dependence of adsorbed Janus discs prior annealing

The height profiles of the particles, which were obtained by section analysis of the SFM height images, reveal an interesting peculiarity. The height profiles exhibit similar shapes, meaning an increase up to a certain level and the development of a plateau (see e.g. Figure 7d in publication). The particles possess high aspect ratios, indicating a very flat geometry. However, during the investigation of various differently crosslinked samples on different substrates it turned out that the plateaus are not always well developed (see Figure S-3). This kind of droplet-shaped appearance was not anticipated for such a polymer brush-like flat particle and deserves further discussion.

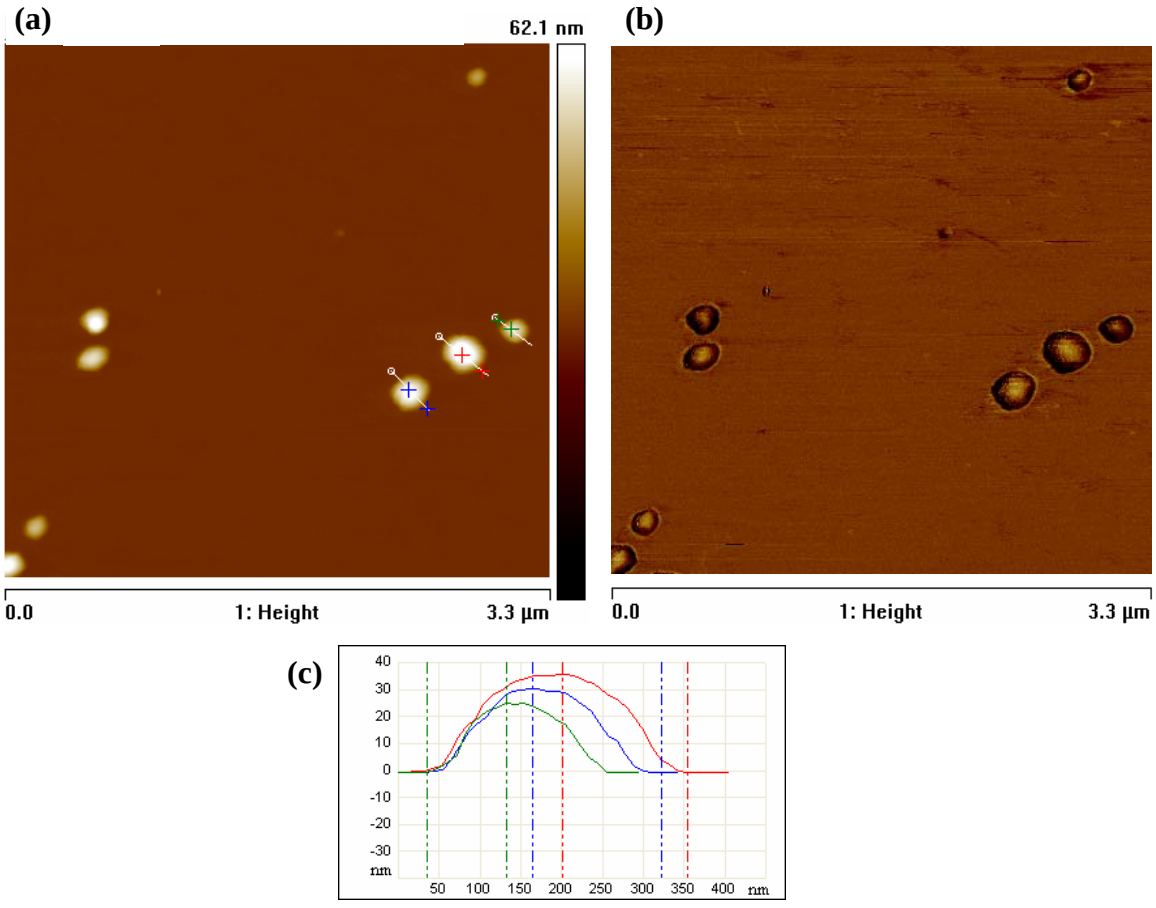

Figure S-3. (a) SFM height image obtained from a sample of Janus discs (SBT-2, 5 wt% AIBN, 5 wt% TRIS, sonication for 5 min at 30% amplitude), dip-coated from a $CHCl_3$ solution (c = 0.1 mg/L) onto mica. (b) Phase image of (a) and (c) section analysis corresponding to the lines shown in image (a).

The phenomenon itself can most frequently be seen for the imaging of samples crosslinked with AIBN using mica as substrate, independent of the block terpolymer template

used. This implies an influence of the substrate and of the crosslinking method, resembling the mechanical strength of the material and the surface energy, respectively. The particles shown in Figure S-3 still possess very high aspect ratios, which can clearly not be caused by any kind of spherical particle or collapsed globule. The presence of vesicles, which might be formed by free lamellae, is also highly improbable, as the observed heights and diameters of the particles are generally too low to fulfil the space requirements for a collapsed unilamellar vesicle ($h_{Vesicle} = 2 \times h_{Janus\ disc} > 45$ nm). Additionally, all samples were prepared from ultradilute solutions (c = 0.1 mg/L), for which aggregates are extremely improbable. Therefore, single flat Janus particles are imaged. A further comparison of the section analyses reveals a dependence of the height of the particles on the overall particle size, meaning that the height increases with rising particle diameter. In order to exclude the presence of any scan artefacts, caused by the finite size of the standard SFM tip (R_{apex} = 10 - 20 nm), images were also recorded with an ultra-sharp tip ($R_{apex} < 2$ nm) but similar height profiles were found.

In order to explain the droplet-like appearance of a part of these particles, one has to consider the sample deposition process and the resulting interfaces. During the deposition of the Janus discs, drying of the solvent takes place and at the end a solvent-swollen disc-like particle is on top of the surface. At all stages of this process the interfacial energy will try to minimize the liquid-air interface and later on, the interface between air and solvent-swollen particle. The most favourable interfacial shape will be that of a droplet. Therefore, in the end of the drying process, the swollen Janus disc adopts the droplet shape, simply to fulfil the energetic conditions of the system. Upon further drying and complete evaporation of the solvent the object is trapped in the droplet-like shape. Hence the structure is kinetically frozen and may not reorient after complete evaporation of the solvent as the thermal energy is insufficient (see scheme S-1).

This drying mechanism can also account for the observed height dependence of differently sized Janus discs. It is expected that a larger Janus disc causes a larger and thus higher droplet at the end of the drying process, thus explaining the difference in the observed height profiles. It is also important to note that the development of a shape similar to that of a droplet may support the formation of very round and smooth border lines of the particles. Small edges or small protrusions could be hidden, however, for large protrusions this cannot be anticipated.

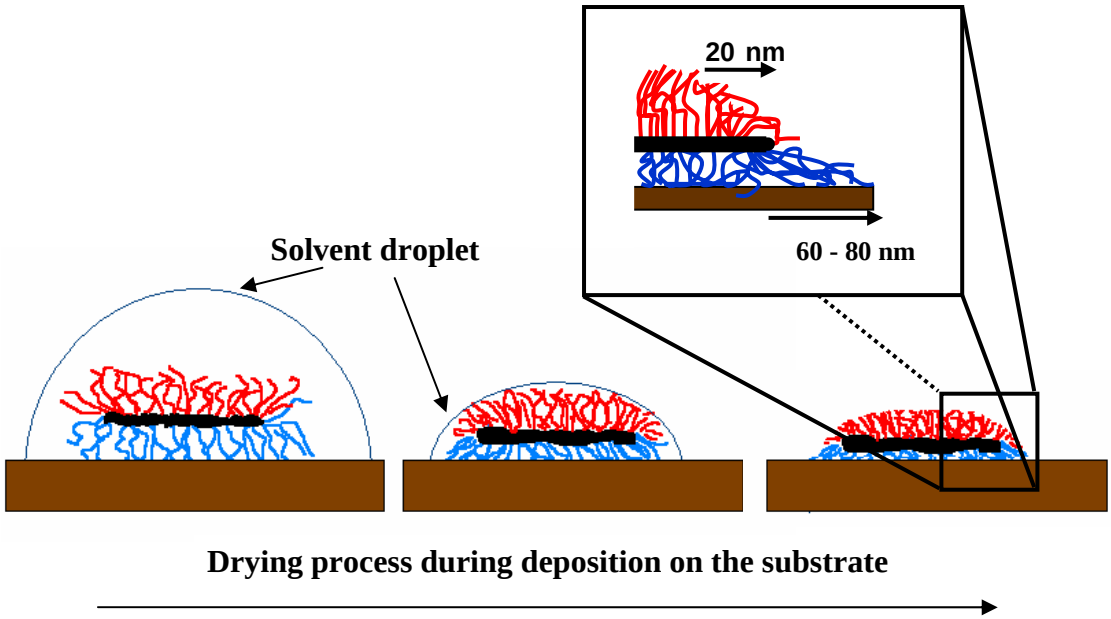

Scheme S-1. Schematic representation of the drying process during deposition of the particles onto the substrate. The red and blue parts indicate PS and P*t*BMA, respectively. The black part corresponds to the inner crosslinked PB layer. The magnified inset displays the expected dimensions of the height increase at an edge of the flat brush-like Janus particle.

To minimize the overall interfacial energy of the totally dry system, the pure Janus disc itself (right-hand side in Scheme S-1) also tries to minimize the interfacial area between the upper PS part and air. A smooth edge with a curved and slow increase in the height profile is thus more favourable than a sharp one, which would be expected for such a brush-like flat particle. In conclusion there is a strong energetic competition between the minimization of the interface and the steric repulsion of the brush hairs of the Janus discs. The latter supports a flat orientation with a sharp height increase whereas the former favours a droplet-like appearance.

In order to prove this assumption and to investigate whether the structures are kinetically frozen, substrates with formerly deposited Janus discs were either heated to 150 °C in vacuo or annealed in toluene vapour (90 °C) in order to allow a thermal relaxation of the particles. Both methods should provide enough energy to allow a segmental movement and a reorientation of the structures. The results obtained are presented within the publication (see figure 11 and text).

5. Cryo-TEM images of very large flat Janus sheets at the onset of the sonication

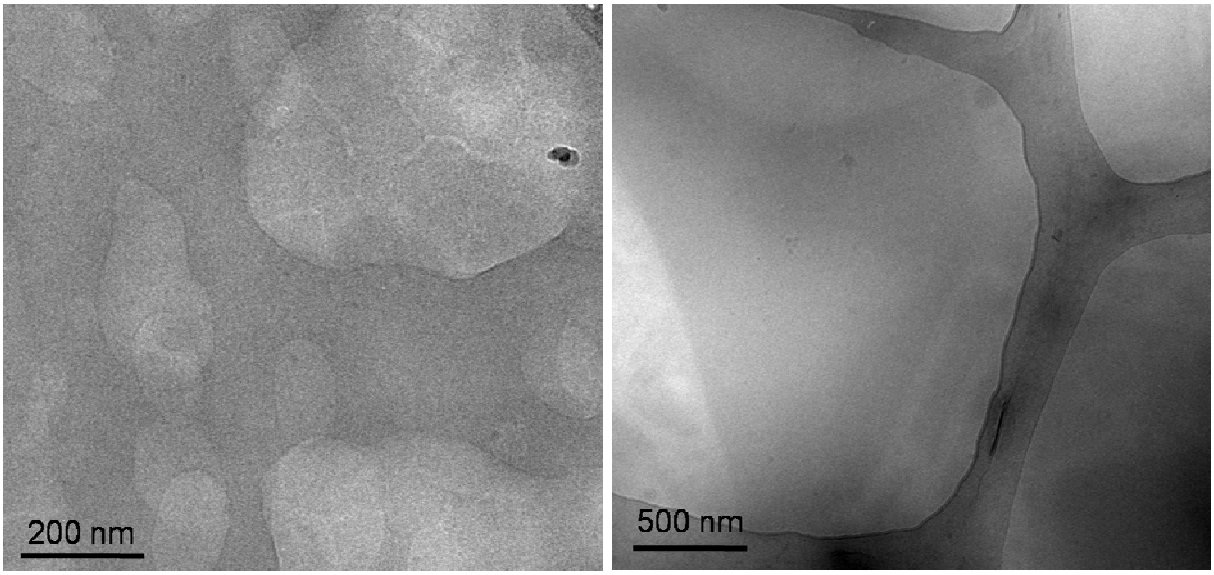

Figure S-4. (a) Cryogenic transmission electron microscopy images of Janus sheets in tetrahydrofuran obtained at the onset of sonication of SBT-2 (left) and SBT-1 (right).

The cryo-TEM image presented on the left above shows a semi-ruptured layer of the crosslinked template, which is characteristic for the beginning of the sonication. At least two layers of the crosslinked template are superimposed onto each other. The image on the right shows a large triangular Janus sheet and some other asymmetric particles on its lower right side (hardly visible). Both samples were filtered prior imaging to remove even larger Janus sheets and some insoluble particles, which can be present at the onset of the homogenization procedure. Similarly semi-ruptured layers and anisometric flat Janus particles cannot be found anymore after prolonged sonication. SFM and cryo-TEM at latter stages show circular particles.

6. Aggregation of Janus discs into layer-like superstructures via back-to-back stacking

The cryo-TEM image shows the aggregation of several small Janus discs. The only way the assembly and the sticking of the several flat particles can take place is via overlapping of several flat particle sides and back-to-back stacking. The section analysis strongly indicates the presence of two layers and a flat geometry in the inside as can be deduced from the step-like profile at the sides and the flat plateau of the grey-scale analyses, respectively.

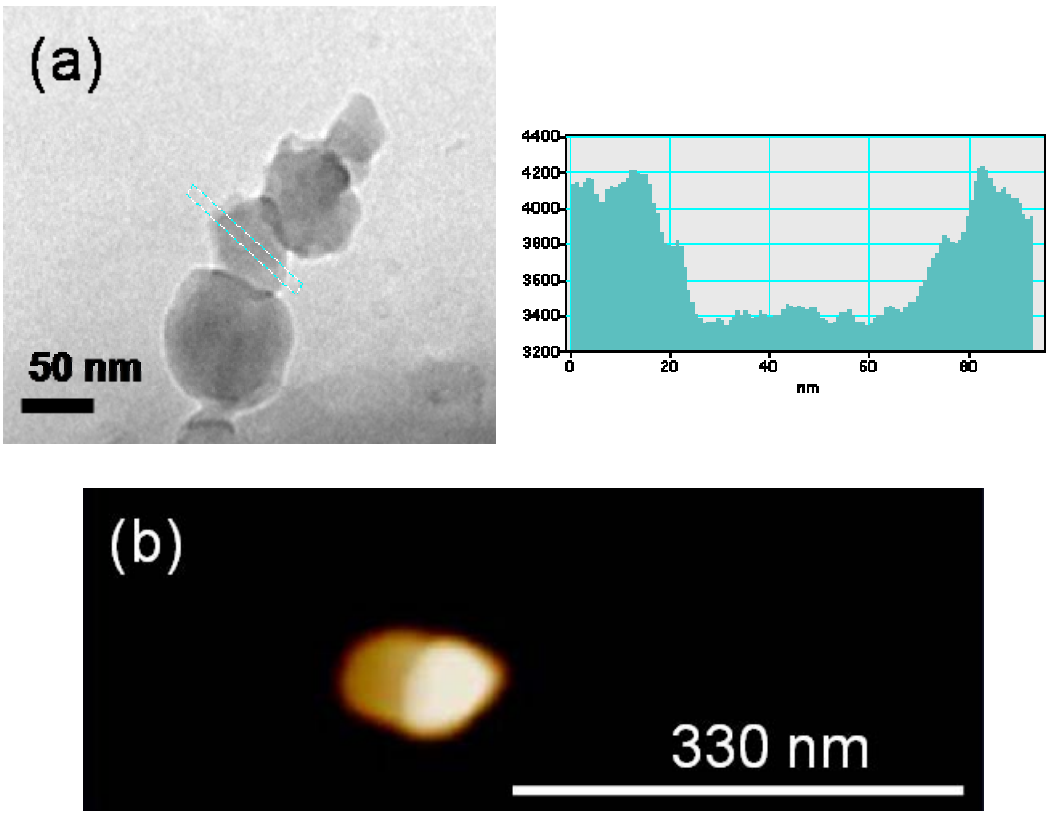

Figure S-5. (a) Cryogenic transmission electron microscopy image of a sample of Janus discs in tetrahydrofuran and its corresponding section analyses. The sample was allowed to equilibrate for several weeks at room temperature before imaging. (b) SFM image of a Janus discs sample (z-scale = 45 nm)

The SFM image below exhibits a back-to-back stacked aggregate. A small Janus disc covers one half of a large flat Janus particle below. Note that the observation of back-to-back stacked aggregates via SFM is not straight-forward as deposition can destroy the loose assemblies and as the SFM deposition was usually done at ultrahigh dilution in order to allow a separation of the particles. At these low dilutions the aggregation tendency of the particles is presumably very low.

References

1. Goldacker, T.; Abetz, V.; Stadler, R.; Erukhimovich, I.; Leibler, L., *Nature* **1999,** 398, (6723), 137-139.
2. Auschra, C.; Stadler, R., *Polymer Bulletin* **1993,** 30, (3), 257-264.
3. Provencher, S. W., *Makromol. Chem.* **1979,** 180, 201.
4. Berne, B. J.; Pecora, R., *Dynamic Light Scattering*. John Wiley & Sons: New York, 1976.
5. Jacobine, A. F., *Radiation Curing in Polymer Science and Technology*. Elsevier Applied Science: London, 1993; Vol. 3, p 219.
6. Decker, C., *Progress in Polymer Science* **1996,** 21, (4), 593-650.
7. Decker, C.; Nguyen Thi Viet, T., *Macromolecular Chemistry and Physics* **1999,** 200, (8), 1965-1974.
8. Decker, C.; Nguyen Thi Viet, T., *Macromolecular Chemistry and Physics* **1999,** 200, (2), 358-367.
9. Decker, C.; Nguyen Thi Viet, T.; Hien Le, X., *Macromolecular Symposia* **1996,** 102, , 63-71.